Extraction of the Model Parameters for the Attenuation in Printed Transmission Lines

Reydezel Torres-Torres, *Member, IEEE*, and Svetlana C. Sejas-García, *Student Member, IEEE*

***Abstract*—A method for determining the parameters of the frequency-dependent attenuation model for transmission lines fabricated on printed circuit boards is presented in this letter. The proposed method allows the separate characterization of the conductor and dielectric losses even when the conductor losses present nonideal variation with frequency. Moreover, the steps for implementing a complete model for a transmission line, including the complex propagation constant and characteristic impedance using the extracted data, are also illustrated. Excellent model-experiment correlation for the complex propagation constant for lines fabricated on a printed circuit board technology is achieved up to 110 GHz.**

***Index Terms*—Attenuation, loss, PCB, transmission lines.**

I. Introduction

THE attenuation constant (α) is an important figure of merit for the interconnects used at the different levels of high-speed electronic systems [1], [2]. In the frequency (f) domain, α can be expressed as the sum of two components: the attenuation associated with the conductor losses (α_c), and that associated with the dielectric losses (α_d). Actually, for the case of a two-conductor transmission line (TL) fabricated on printed circuit board (PCB) technology operating at microwave frequencies, the widely used attenuation model dictates that α_c and α_d are approximately proportional to $f^{0.5}$ and f respectively [3]. Based on this fact, a technique for separating the conductor and dielectric losses in PCB TLs was reported in [4]. However, the ideal f-dependent model for α_c fails to reproduce experimental data above a certain frequency and poor agreement between simulated and experimental data is obtained beyond this limit. For this reason, a modified model for α_c has been applied to TLs on semiconductor [1] as well as on PCB substrates [2], in which the typical dependence on $f^{0.5}$ is substituted by a dependence on f^n. This modified model allows the proper correlation of simulated with experimental data within a wide frequency range.

This letter presents an approach for determining the model parameters for α including the exponent n that is required for the modeling of the conductor losses. Afterwards, physically-based f-dependent models are implemented for the per unit resistance (R), inductance (L), conductance (G), and capacitance (C) (i.e., the *RLGC* parameters) of PCB TLs. This allows to represent the corresponding propagation constant $(\gamma = \alpha + j\beta)$ and characteristic impedance (Z_c) up to 110 GHz.

Manuscript received June 25, 2010; revised August 23, 2010; accepted September 15, 2010. Date of publication November 01, 2010; date of current version December 03, 2010. This work was supported in part by Intel Corporation and CONACyT-Mexico under Grants 118818 and 213385.

The authors are with the Instituto Nacional de Astrofísica, Óptica y Electrónica (INAOE), Department of Electronics, Tonantzintla, Puebla 72840, Mexico (e-mail: reydezel@inaoep.mx).

Color versions of one or more of the figures in this letter are available online at http://ieeexplore.ieee.org.

Digital Object Identifier 10.1109/LMWC.2010.2080355

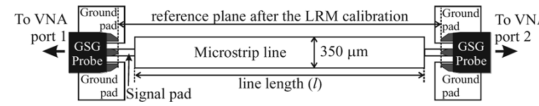

Fig. 1. Sketch illustrating the layout of the fabricated microstrip lines. Notice also the configuration of the probing pads for measuring S-parameters.

II. Experiments

Fig. 1 shows the layout of the TLs used for illustrating the development and verification of the proposed method. These lines were fabricated on a PCB made of a low-loss Rogers RT/Duroid 5880 material, with a thickness of 127 μm, and nominal relative permittivity (ε_r) and loss tangent $(\tan\theta)$ of 2.2 and 0.0017, respectively. The lines were made of copper with a thickness (t) of 36 μm and the substrate—metal interface presents a nominal root mean square roughness (h_{rms}) of 1.8 μm. Fig. 1 shows that the lines have a width (w) of 350 μm, different lengths (l), and are terminated with ground-signal-ground (GSG) pads so that coplanar RF-probes with a pitch of 150 μm can be used to perform S-parameter measurements. These measurements were carried out using a vector network analyzer (VNA) which was calibrated up to the probe tips by using a line-reflect-match (LRM) algorithm and an impedance-standard-substrate (ISS) provided by the probe manufacturer. Afterwards, γ (per meter) was determined from the experimental data of two lines with $l = 12.7$ mm and 25.4 mm by applying a line-line procedure that removes the effect of the parasitics associated with the pads shown in Fig. 1 [5].

III. Parameter Determination for the Attenuation

A detailed f-dependent model for the attenuation occurring in TLs is described in [3]. Assuming that $\tan\theta \ll 1$, such as in the case of typical PCB substrates, the model is reduced to [4]

$$\alpha = k_1 f^{0.5} + k_2 f \tag{1}$$

where k_1 and k_2 are constants. Thus, in accordance to (1), these constants can be respectively obtained from the intercept with the ordinates and the slope of the linear regression of the experimental $\alpha/f^{0.5}$ versus $f^{0.5}$ curve.

Fig. 2 shows the extraction of k_1 and k_2 for the fabricated lines. Notice that the linear regression allows to represent the experimental data up to about 20 GHz. For higher frequencies, however, (1) is no longer valid and the regression deviates from the data. Hence, an alternative model is necessary for α, in which α_c is assumed to be proportional to f^n, where n is a positive real number. In this case, α can be written as

$$\alpha = K_1 f^n + K_2 f. \tag{2}$$

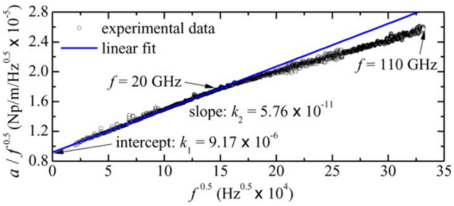

Fig. 2. Determination of the parameters in (1). A single linear regression fails for representing the data for the measured frequency range (up to 110 GHz).

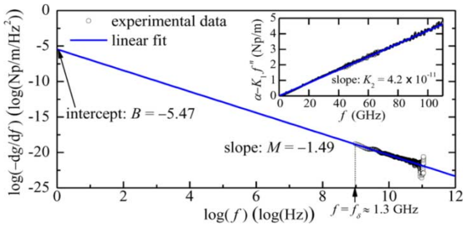

Fig. 3. Regressions used to determine the attenuation model parameters using the new method for the fabricated lines from 1 to 110 GHz.

Even though K_1 and K_2 are constants, the introduction of the third unknown parameter n increases the difficulty of the parameter extraction since (2) cannot be written so that a simple linear fit of experimental data is performed. However, this problem can be solved as described as follows.

Equation (2) can be rewritten as

$$g = K_1 f^N + K_2 \tag{3}$$

where $g = \alpha/f$ and $N = n - 1$. The derivative of g is given by

$$\frac{dg}{df} = N K_1 f^{N-1} \tag{4}$$

which allows to reduce the number of unknown parameters to two. Then, multiplying by -1 and applying the logarithm (with base 10) to both sides of (4) yields

$$\log\left(-\frac{dg}{df}\right) = \log(-NK_1 f^{N-1}). \tag{5}$$

In accordance to (3), since $0 < n < 1$ then $N < 0$ and g is a monotonically decreasing function of f. In consequence, dg/df is negative, which makes necessary the use of the minus signs in (5) for the logarithms to be real numbers.

Using logarithmic identities, (5) can be expanded as

$$\log\left(-\frac{dg}{df}\right) = \log(-NK_1) + (N-1)\log(f) \tag{6}$$

which allows to respectively determine $\log(-NK_1)$ and $(N-1)$ from the intercept with the ordinates, B, and the slope, M, of the linear regression of the experimental $\log(-dg/df)$ versus $\log(f)$ curve. Thus, K_1 and n in (2) can be obtained using

$$K_1 = -\frac{10^B}{(M+1)} \tag{7}$$

$$n = M + 2 \tag{8}$$

Once K_1 and n are known, (2) can be solved for $\alpha_d = K_2 f$, which allows to determine K_2 from the slope of the linear regression of the $(\alpha - K_1 f^n)$ versus f data. This regression, as well as that associated with (6) is shown in Fig. 3.

In order to apply the linear regression defined by means of (6), the experimental dg/df has to be obtained. In this regard, it is well known that differentiating using finite-difference approaches greatly amplifies the noise associated with experimental data. Due to this, we applied an alternative differentiation algorithm described in [6] to accurately obtain dg/df. In this case, an excellent linear trend of the experimentally determined data is observed in Fig. 3, which allows to easily obtain the following values for the fabricated lines: $K_1 = 7 \times 10^{-6}$, $K_2 = 4.2 \times 10^{-11}$, and $n = 0.52$.

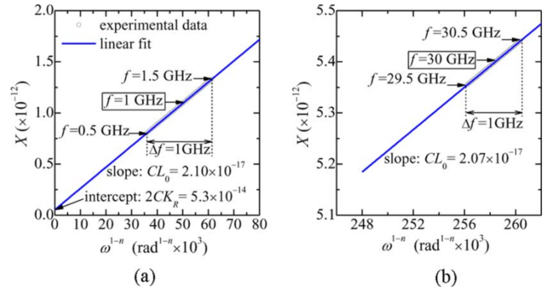

Fig. 4. Determination of CL_0 at $f = 1$ GHz (left) and $f = 30$ GHz (right).

In [3], obtaining $n > 0.5$ is attributed to the effect of the roughness of the substrate—metal interface, which starts becoming apparent when f increases to around f_δ, defined as the frequency at which the skin depth of the metal (δ) equals h_{rms}. For considering this effect, k_1 in (1) can be modeled including an f-dependent term. When $f \gg f_\delta$, however, this term becomes weakly dependent on f [7]. Thus, since the fabricated lines present $f_\delta \approx 1.3$ GHz, it is expected that the dependence of k_1 with f is relatively weak at 20 GHz. Notice, however, in Fig. 2 the accentuated variation in α around this frequency, which indicates the combined influence of the roughness with another effect. This effect is the variation in the distribution of the current within the cross section of the metal lines, which is dependent on f and is accentuated when t is comparable to w in microstrip lines [8]. Full-wave simulations of the current distribution in the cross-section of the studied TLs indicate that, around 20 GHz, most of the current in the signal trace flows at the bottom and at the sidewalls, increasing the value of k_1 as compared to that seen at relatively low frequencies (i.e., when considerable part of the current also flows at the top of the line). The combined impact of these effects on R is quantified in Section IV.

IV. Implementation of a Transmission Line Model

This section focuses on implementing a model for the *RLGC* parameters of a TL assuming quasi-TEM mode propagation and using the extracted n.

Neglecting the low-frequency resistance and conductance is valid for PCB TLs since $\delta \ll t$ the skin depth is much smaller than the trace thickness at microwave frequencies and the dielectric leakage currents are very small. Thus, assuming that α_c is proportional to f^n, the *RLGC* parameters can be represented by using a causal model as [9]

$$R = K_R \omega^n \tag{9}$$

$$L = L_0 + K_R \omega^{n-1} \tag{10}$$

$$G = \omega C \tan\theta_{eff} \tag{11}$$

where K_R and L_0 are constants, whereas C and the effective loss tangent $(\tan\theta_{eff})$ are dependent on f for the model to be causal. For simplicity, we used here $\omega = 2\pi f$.

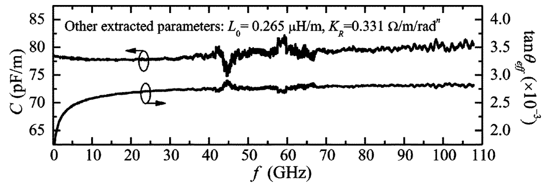

Fig. 5. Extracted parameters for implementing the *RLGC* model.

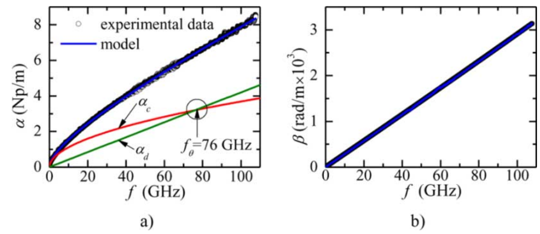

Fig. 6. Simulation-experiment comparison for: a) α, and b) β.

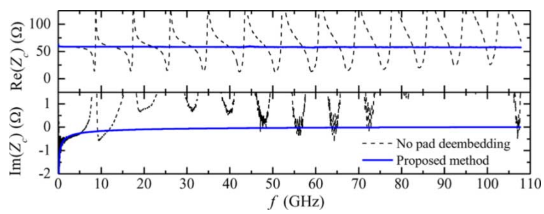

Fig. 7. Comparison between Z_c obtained using the extracted parameters and directly obtained using the data of the fabricated line with $l = 12.7$ mm [11].

To obtain the parameters in (9)–(11), γ is expressed as

$$\gamma = \alpha + j\beta = \sqrt{ZY} \tag{12}$$

where $Z = R + j\omega L$, $Y = G + j\omega C$, and $j^2 = -1$. Thus, substituting (9)–(11) into (12) and assuming $\tan\theta_{eff} \ll 1$ yields

$$X = \frac{\mathrm{Im}(\gamma^2) - \mathrm{Re}(\gamma^2)}{\omega^{n+1}} = 2CK_R + CL_0\omega^{1-n}. \tag{13}$$

Hence, the term CL_0 can be determined from the slope of the linear regression of the experimental X versus ω^{1-n} curve. However, since C depends on f the regression has to be performed at intervals at which the variation of this parameter is small, which is achievable due to the weak dependence of C with f for PCB TLs [10]. Fig. 4 shows the extraction of CL_0 at two different frequencies showing good linearity considering a frequency interval of 1 GHz; notice also that $2CK_R$ is obtained from the intercept with the ordinates. Afterwards, K_R can be determined at low frequencies from $2CK_R/2C_0$, where C_0 is the DC capacitance of the line [10]; L_0 is found in a similar way, whereas C is obtained from CL_0/L_0.

To complete the extraction, $\tan\theta_{eff}$ is obtained from

$$\tan\theta_{eff} = \frac{\mathrm{Im}(\gamma^2) - CK_R\omega^{n+1}}{CL_0\omega^2 + CK_R\omega^{n+1}}. \tag{14}$$

Fig. 5 shows the extracted parameters, which allow to accurately representing γ as shown in Fig. 6. This figure also shows the curves for $\alpha_c = K_1 f^n$ and $\alpha_d = K_2 f$, as well as the crossover frequency f_θ, which is the frequency at which $\alpha_d = \alpha_c$. As is well known, f_θ is dependent not only on the material properties but also on the structure and dimensions of the TLs. Analytically, f_θ can be calculated as

$$f_\theta = \left(\frac{K_1}{K_2}\right)^{1/(1-n)}. \tag{15}$$

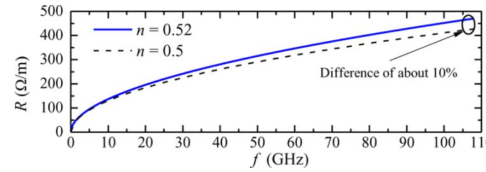

Fig. 8. Simulated R curves assuming $n = 0.5$ and $n = 0.52$ in the model for α.

Notice that other than the experimental γ, no additional data is required for applying the proposed method. This is convenient because the accurate determination of Z_c at high-frequencies represents a challenge [11]. Hence, we propose obtaining $Z_c = \sqrt{Z/Y}$ using (9)–(11) and the extracted parameters. Fig. 7 shows the result, where the fluctuations introduced by the effect of the pad parasitics are not observed.

Finally, R is plotted versus f in Fig. 8 using (9) and $n = 0.52$. As can be seen, R is about 10% higher when compared with the model obtained assuming $n = 0.5$ and carrying out the parameter extraction using data up to 20 GHz. This result points out the importance of considering additional effects in α_c when implementing wideband TL models.

V. Conclusion

A method to obtain the attenuation model parameters for PCB transmission lines has been presented and demonstrated up to 110 GHz. The method allows the implementation of a model for the fundamental parameters of a transmission line. Moreover, the frequency at which the dielectric losses surpass the conductor losses can also be obtained using the extracted parameters. The extraction technique is simple and analytical, allowing the modeling of transmission lines for circuit design and deembedding purposes.

References

[1] G. Ponchak *et al.*, "Low-loss CPW on low-resistivity Si substrates with a micromachined polyimide interface layer for RFIC interconnects," *IEEE Trans. Microw. Theory Tech.*, vol. 49, no. 5, pp. 866–870, May 2001.

[2] J. A. McCall and D. Shykind, "Nonideal frequency dependent loss in realistic PCB transmission lines," in *Proc. IEEE Workshop Signal Prop. Interconnects*, May 2002, pp. 79–82.

[3] H. Johnson and M. Graham, *High Speed Signal Propagation: Advanced Black Magic*. Englewood Cliffs, NJ: Prentice-Hall, 2003.

[4] R. Torres-Torres and V. H. Vega-Gonzalez, "An approach for quantifying the conductor and dielectric losses in PCB transmission lines," in *Proc. IEEE EPEPS*, Nov. 2009, pp. 235–238.

[5] J. A. Reynoso-Hernández, "Unified method for determining the complex propagation constant of reflecting and nonreflecting transmission lines," *IEEE Microw. Wireless Compon. Lett.*, vol. 13, no. 8, pp. 351–353, Aug. 2003.

[6] J. J. Stickel, "Data smoothing and numerical differentiation by a regularization method," *Comput. Chem. Eng.*, vol. 34, pp. 467–475, Apr. 2010.

[7] A. F. Horn *et al.*, "Effect of conductor profile on the insertion loss, phase constant, and dispersion in thin high frequency transmission lines," *DesignCon*, pp. 1–22, 2010.

[8] B. Curran *et al.*, "A methodology for combined modeling of skin, proximity, edge, and surface roughness effects," *IEEE Trans. Microw. Theory Tech.*, vol. 58, no. 9, pp. 2448–2455, Sep. 2010.

[9] J. Zhang *et al.*, "Causal $\mathrm{RLGC}(f)$ models for transmission lines from measured S-parameters," *IEEE Trans. Electromagn. Compat.*, vol. 52, no. 2, pp. 189–198, Feb. 2010.

[10] R. B. Marks and D. F. Williams, "Characteristic impedance determination using propagation constant measurement," *IEEE Microw. Guided Wave Lett.*, vol. 1, no. 6, pp. 141–143, Jun. 1991.

[11] J. E. Post, "On determining the characteristic impedance of low-loss transmission lines," *Microw. Opt. Technol. Lett.*, vol. 47, pp. 176–180, Oct. 2005.